10-GHz 1.59 μm quantum dash passively mode-locked two-section lasers

M. Dontabactouny[a], C. Rosenberg[b], E. Semenova[b], D. Larsson[b], K. Yvind[b], R. Piron[a], F. Grillot[a], O. Dehaese[a] and S. Loualiche[a]

[a]Université Européenne de Bretagne, CNRS – Laboratoire FOTON UMR 6082, INSA Rennes, 20 av des buttes de Coësmes, 35043 Rennes, France

[b]Department of Photonics Engineering, Technical University of Denmark, Ørsteds Plads, 2800 Kongens Lyngby, Denmark

ABSTRACT

This paper reports the fabrication and the characterisation of a 10 GHz two-section passively mode-locked quantum dash laser emitting at 1.59 μm. The potential of the device's mode-locking is investigated through an analytical model taking into account both the material parameters and the laser geometry. Results show that the combination of a small absorbing section coupled to a high absorption coefficient can lead to an efficient mode-locking. Although output pulses are found to be chirped noise measurements demonstrate that the single side band phase noise does not exceed -80 dBc/Hz at 100 kHz offset leading to an average timing jitter as low as 800 fs. As compared to single QW lasers these results constitute a significant improvement and are of first importance for applications in optical telecommunications.

Keywords: quantum dots/dashes, ultra-fast lasers, mode-locking

1. INTRODUCTION

Monolithic passively mode-locked laser (MLL) diodes are highly interesting for ultra high bit rate optical telecommunications for the achievement of all optical systems for clock recovery, clock distribution, optical sampling so as to overcome the bandwidth limitations of high end electronic systems at reasonable cost. The first semiconductor MLL was realised using bulk active material system with an ion implanted saturable absorber (SA) [1]. Soon after mode-locking was achieved using quantum well (QW) active material allowing improved performances [2]. State of the art QW MLLs have demonstrated some performance such as a pulse repetition rate as large as 860 GHz [3]. Although QW have been used for a long time, the inclusion of quantum dots (QD) or dashes (QDH) in the active zone has been predicted to lead to a lower threshold current, a narrower spectral emission and a reduced temperature sensitivity [4, 5]. On one hand these improvements are mainly attributed to the modified density of state (DOS) provided with the higher dimensional carrier confinement. Because the modified DOS results in an increased ratio of saturation energies between the gain and SA sections, a better stability of the mode-locking is expected [6]. On the other hand the reduced active volume due to dimensional confinement allows a lower coupling with the lasing mode decreasing the amplified spontaneous emission (ASE) and as a result the noise [7]. Furthermore due to their inhomogeneous size distribution, QD actually exhibit a broader spectral emission as compared to their QW counterparts which is an advantage for the generation of ultra-short pulses. The first demonstration of a QD MLL was done on GaAs substrate with a pulse repetition rate of 7.4 GHz [8]. Since then, InGaAs/GaAs QD MLLs with frequencies from 300 MHz to 200 GHz, pulse durations from 10 ps to 400 fs, and peak powers beyond 2W have been reported [9]. Development of InAs/GaAs QD lasers is mostly suitable for short-haul telecommunications for which an emission wavelength located in the 1-1.3 μm is required. However, in order to reach the standards of long-haul communications, 1.55 μm emission wavelength is mandatory. The longest emission wavelength achieved with InAs/GaAs QD lasers is 1.46 μm though with a high threshold current [10]. Therefore much attention is now devoted to QD gown on InP substrate. Achievements of passive mode-locking based on InAs/InP quantum nanostructures have led to pulse repetition rate as high as 346 GHz [11]. Fourier limited subpicosecond pulses down to 312 fs [12] have also been reported on single section lasers. Heck et al. recently have reported passive mode-locking in two-section InAs/InP QD lasers up to 10.5 GHz at 10°C [13, 14].

While mode-locking condition in single section lasers is inherent to the material itself, multi section lasers have at least one section used as an SA so as to produce the mode-locking. Thus, through the absorber to gain length ratio defined during mask processing and the reverse bias voltage applied to the SA, the mode-locking performance could be altered to

meet a specific requirement. Moreover by modulating the current in the SA with the same period as the cavity round trip time, hybrid mode-locking can be achieved leading usually to a reduced jitter [15]. This paper reports the fabrication and the characterisations of a 10.6 GHz two-section passively mode-locked QDH laser emitting at 1.59 μm. The potential of the device's mode-locking is investigated through an analytical model taking into account both the material parameters and the laser geometry [16]. Results show that the combination of a small absorbing section coupled to a high absorption coefficient can lead to an efficient mode-locking operation with pulse widths as low as 1.5 ps. Noise measurements also demonstrate that the single side band phase noise is as low as -80 dBc/Hz at 100 kHz offset while the average timing jitter does not exceed 800 fs. As compared to single QW lasers these results constitute a significant improvement and are of first importance for applications in optical telecommunications.

2. DEVICE DESIGN

2.1 Epitaxial structure

The investigated semiconductor structure was grown by gas source molecular beam epitaxy (GSMBE) on highly n doped InP (100) substrate. The active material consists of 5 layers of InAs QDH grown using the double cap method [17]. The latter consists in growing the capping layer over the dashes in two steps separated by a growth interruption under phosphorus flux to reduce the height of the dashes and to control the emission wavelength. As a result the carrier lifetime is increased from about 700 ps [18] to 1600 ps [19] which could be due to a lowered number of defects when stacking several layers. As a consequence of that, the laser's threshold current is decreased [20, 21]. The capping layers consist in 20 nm thick phosphide quaternary alloy with a gap wavelength of 1.18 μm (PQ(1.18)) layers. The stack is centred in a 320 nm thick waveguide of PQ(1.18). The cladding is realised by 300nm thick n type and p type InP layers respectively below and above the PQ(1.18). The whole structure is described in the figure 1.

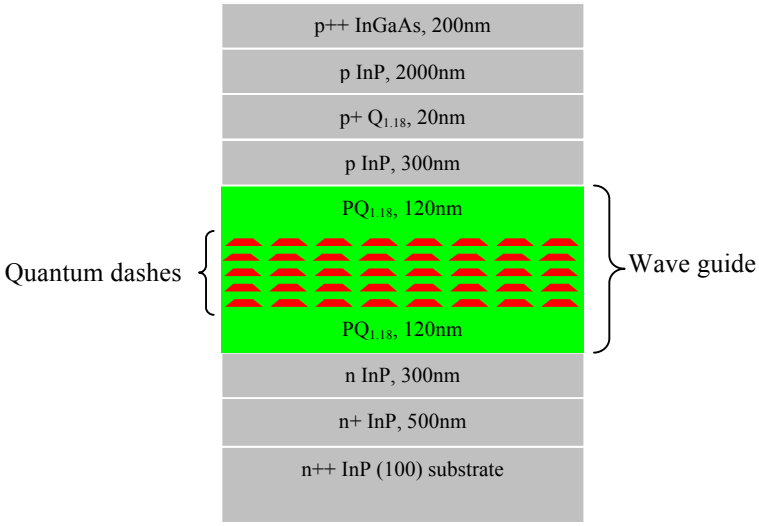

Figure 1: Epitaxial structure of the investigated quantum dashes (the '+' sign denotes a higher concentration of dopants and '++' an even higher one)

2.2 Laser device design

As shown in figure 2 the fabricated devices are edge emitting Fabry Perot two-section ridge lasers. In order to measure modal gain and loss, segmented semiconductor optical amplifiers (SOA) are also fabricated. The ridge width is about 2 μm and the etching was done until about 100 nm of p type InP is left above the waveguide. The thickness to be left was determined by simulation software using the Marcatili method so as to lead to single modal guiding with the optimum confinement. To create electrical isolations between sections, 5 μm separations along the ridges were done by etching the contact layer and 200 nm into the p type InP buffer layer. The depth of etch is chosen to be enough to have a resistance of about 2 kΩ. The length of the SA section is about 3.2% the total length of the laser which is 4 mm. The Bisbenzocyclobutene (BCB), an electrical insulator with low dielectric strength was then used for planarization of the surface. P and n contact metallization were done with e-beam. The device was then mounted for easy handling on a

metal plated epoxy substrate with gold tin alloy. Finally the SA side facet was coated with silver for high reflectivity so as to create self colliding effect in the SA.

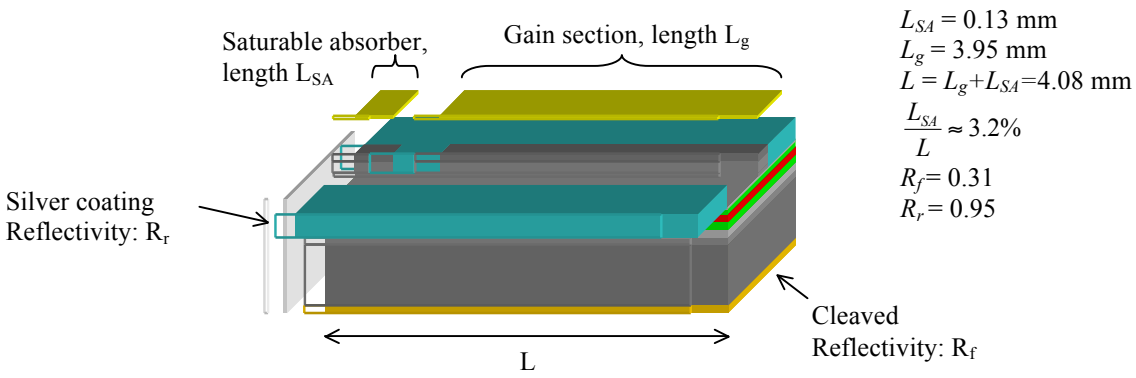

Figure 2: Laser device schematics

3. DEVICE CHARACTERISATION

3.1 Characterisation set-up

The device was placed on a copper block maintained at 20 °C by means of a thermo electric cooler (TEC). The output of the laser was coupled to a single mode fibre through an anti-reflection coated lensed isolator and distributed to 4 outputs. One with 85% of the total output power further amplified by an L-band amplifier (L-EDFA) for autocorrelation (AC), the three others with 5% each for the power meter (PM), the RF/electrical spectrum analyser (ESA) (22 GHz bandwidth) and the optical spectrum analyser (OSA) (10 pm resolution). A direct voltage generator is used for reverse biasing the SA and a direct current generator for forward biasing the gain section. The characterisation set-up is described in figure 3.

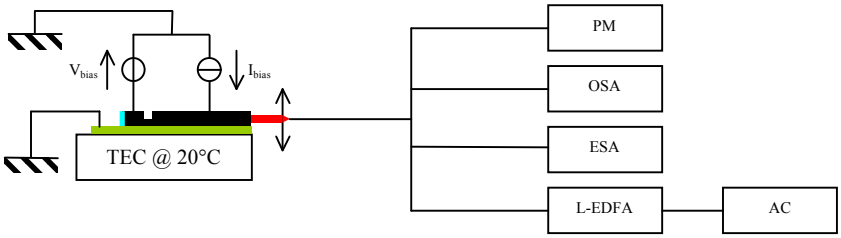

Figure 3: Characterisation set-up diagram

3.2 Theoretical discussion

An analytical model has been used to theoretically analyse the mode-locking potential of the given two section laser. The model was originally derived by Lau and Palaski [22, 23] for two section passively mode-locked lasers without self-pulsation. However, as pointed out by Lin et al., this model holds under the assumption that the gain and the passive absorber are distributed uniformly in the optical cavity. As a consequence of that, an extension has been proposed by taking into account a gain section of length L_g and an absorber section of length L_a. Similar to Lau and Palaski's model, the net gain modulation can be re-written such as [16]:

$$g_{net} = \left(\frac{-G_g g_0 L_g}{i\omega + 1/T_g} - \frac{G_a a_0 L_a}{i\omega + 1/T_a} \right) \frac{s e^{i\omega t}}{L} = \hat{g}_{net} e^{i\omega t} \qquad (1a)$$

$$1/T_g = 1/\tau_g + G_g S_0 \qquad 1/T_a = 1/\tau_a + G_a S_0 \tag{1b}$$

$$G_g = \upsilon_g \frac{dg_0}{dn} \qquad G_a = \upsilon_g \frac{da_0}{dn} \tag{1c}$$

$$S_0 = \frac{1}{\alpha_m \upsilon_g h\nu} \frac{\Gamma P}{WdL} \tag{1d}$$

In the set of equations (1a)-(1d), g_0, a_0, dg_0/dn and da_0/dn are the modal gain, the unsaturated absorption, the differential gain and the differential absorption, n being the carrier density. The circular frequency $\omega = 2\pi F$ refers to the laser's roundtrip frequency F while s corresponds to the real amplitude of the oscillation and t is time. T_g, T_a, τ_g and τ_a are the effective and spontaneous lifetimes in the gain and absorber sections respectively. Other device's parameters such as S_0, υ_g, α_m, $h\nu$, W and Γ denote the average photon density in the cavity, the peak power, the group velocity in the waveguide, the mirror loss, the photon energy, the lateral mode width and the optical confinement factor.

In order to ensure mode-locking, the real part of the net gain described through equation (1a) must exceed the internal loss of the waveguide. Assuming this condition as well as a power sufficiently large, analytical derivations lead to a relationship for mode-locking operation such as:

$$\frac{a_0}{g_0}\frac{L_a}{L_g} > \left(\frac{\frac{dg_0}{dJ}}{\left.\frac{dg_0}{dJ}\right|_{g_0=0}} \right)^2 \tag{2}$$

In inequality (2), the amounts dg_0/dJ and $(dg_0/dJ)_{g0=0}$ are respectively the differential gain and the differential absorption with respect to the pump current density J. The differential gain is calculated at the given pumping condition while the differential absorption is assumed to be equal to the differential gain at the transparency. This inequality gives the operating requirements for a two section passively mode-locked laser and highlights the interdependence between the material parameters and the device geometry. Amounts g_0, a_0, (dg_0/dJ), $(dg_0/dJ)_{g0=0}$ are measured using the segmented contact method based on the use of multi section ridge SOA waveguides [24].

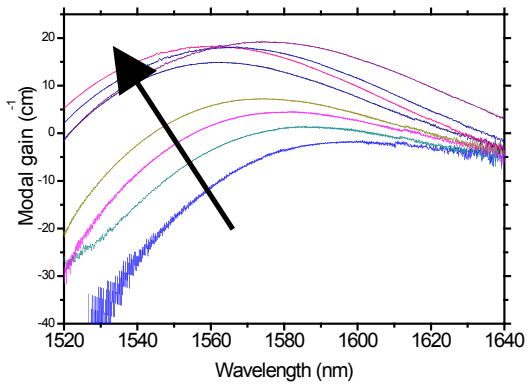

Figure 4: The modal gain spectra for different pump current densities. The black arrow represents the increase of the pumping conditions

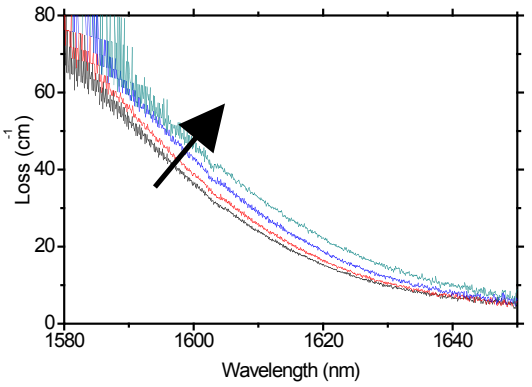

Figure 5: The loss spectra for different values of the reverse bias voltage. The black arrow represents the increase of the reverse bias

The figure 4 represents the SOA modal gain spectra for the following pump current densities 714, 952, 1190, 1428, 2380, 4760, 7140 and 11900 A.cm^{-2}. The chosen operating current of the laser for characterization is about 250 mA corresponding to a 3 kA.cm^{-2} current density while the reverse bias voltage applied to the SA is 1.6 V. As shown later lasing peak is observed at 1594 nm. All the parameters needed for the model are referenced in table 1. The measured modal gain is about 11 cm^{-1} at 3 kA.cm^{-2} while it gets clamped around 20 cm^{-1} at higher injection rates. The figure 5 represents the

evolution of the loss as a function of the wavelength for the following values of the reverse bias voltage 0V, 1V 2V and 3V. As it can be seen the loss decreases abruptly for wavelengths far from the emission peak at low pump current and tends to a constant value. Around the emission peak the high absorption is due to the quantum electronic gap of the QDH while far from that wavelength the absorption is due to the internal loss of the waveguide. Thus, the unsaturated absorption a_0 is calculated by subtracting internal loss α_i from the total loss at the laser operating wavelength $\alpha(\lambda)$. The figure 6 shows the measured modal gain at 1594 nm as a function of the current density. The red solid line corresponding to the modal gain curve-fitting conducted through an exponential fit [25] is used to estimate differential gains (dg_0/dJ) and $(dg_0/dJ)_{g0=0}$ via its derivative as shown in figure 7.

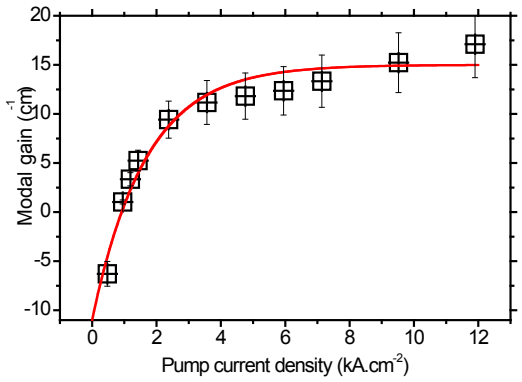

Figure 6: Modal gain vs. pump current density for the laser's operating wavelength of 1594nm. Experimental data (squares) and fit (red line)

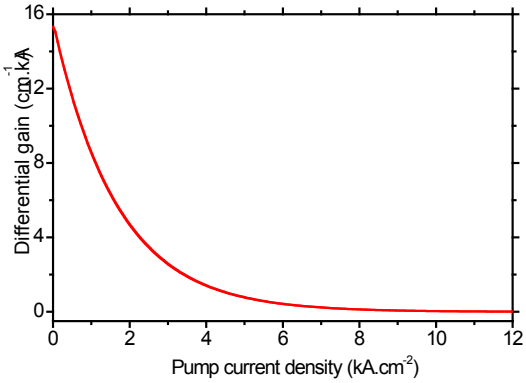

Figure 7: Calculated differential gain vs. pump current density

Parameter	Value	units
L_a	130	µm
L_g	3950	µm
L	4080	µm
α_i	6	cm^{-1}
α_m	1.5	cm^{-1}
a_0	50	cm^{-1}
g_0	11	cm^{-1}
Left member inequality.(2)	**0.15**	
Right member inequality.(2)	**$8\ 10^{-2}$**	
Inequality (2) satisfied	**Yes**	

Table 1: list of parameter values used in the model

Calculations reported in table 1 show that the inequality (2) is satisfied, meaning that the given two-section laser should get mode-locked at the given current under study. It should be noted that associated to inequality (2) is the threshold condition, which can be written such as:

$$g_0 L_g = a_0 L_a + (\alpha_m + \alpha_i) L \qquad (3)$$

The calculated value of g_0 from (3) is 9.4 cm^{-1} which corresponds from figure 6 to a pump current density of 2.5 $kA.cm^{-2}$. Using this value, inequality (2) is found to be weakly satisfied. However, the operating condition chosen for this study remaining close to 2.5 kA cm^{-2}, inequality (2) is considered to be satisfied over the range of current under study.

These results are interesting because they point out that mode-locking should be possible when properly combining a shorter SA section and a larger absorption coefficient.

3.3 Laser performances

The threshold current was measured through light current characteristics shown in figure 8. Under CW current injection the threshold is 71 mA, while it is about 77 mA with low variation when the SA was reversely biased with voltages between 0 and 4 V. For all the measurements presented in this paper the input gain current was set as said earlier to 250 mA to achieve a high output power. The reverse bias voltage over the SA when on, was set to 1.6 V corresponding to the point at which the RF peak reached its highest value.

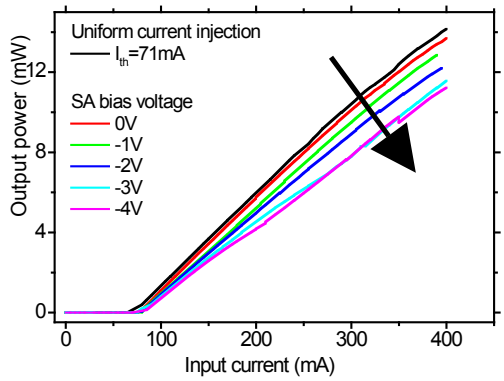

Figure 8: Light-current characteristics as a function of different reverse bias voltages. The black arrow represents the increase of the reverse bias

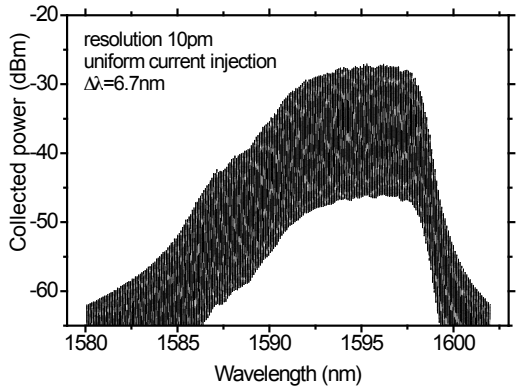

Figure 9: Optical spectrum under 250mA uniform injection

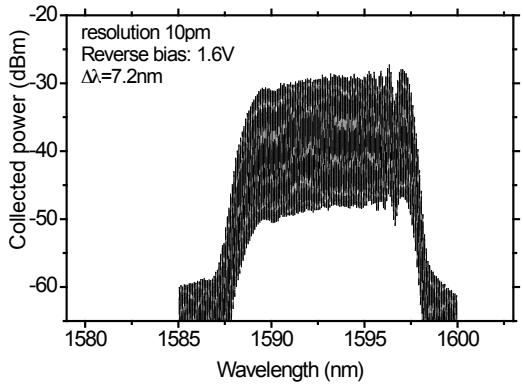

Figure 10: Optical spectrum under 250mA in gain section and SA 1.6V reverse biased

The figure 9 shows the optical spectrum under uniform current injection. The line peaks at 1597 nm with a width of 6.7 nm. When the reverse bias is on, the peak centre moves to 1594nm and the linewidth increases to 7.2 nm as seen in the figure 10. In the latter case the appearance of smooth bumps on part of the optical spectrum indicates that partial mode locking is happening. However no pulse could be seen in the autocorrelation or on a fast oscilloscope.

To further investigate the laser signal a 1nm bandwidth filter centred at 1600 nm tuneable on a window of 20 nm was used at the output of the laser signal. Autocorrelation led to the measurement of pulses ranging from 8 to 14 ps depending on the position of the filter. Figure 11 show that the shortest pulses were measured at the extreme left and right parts of the spectrum.

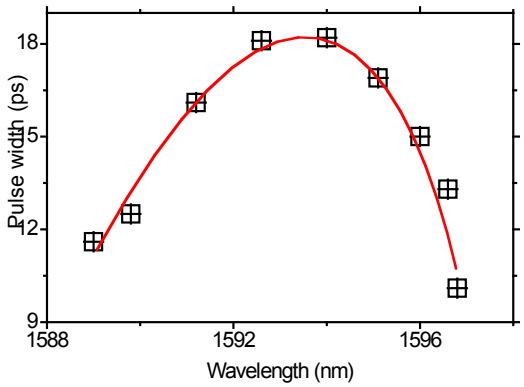

Figure 11: Pulse width vs. filter wavelength (dots) with eye guide (red line)

In figure 11 the pulse width depicted as a function of the wavelength seems to match with the characteristics of strongly linear chirped pulses. Indeed on a linearly chirped radiation a spectral filter is equivalent to a window in the time domain. Thus the measured pulsewidth is directly related to the size of the overlapping region between the pulse and the temporal window. Selecting the edges of the spectral line of the mode-locked region would let pass only the edges of the pulses which yields short pulse measurements with the autocorrelator. The longest pulses are measured when the temporal window centre matches with the pulses peak. In the case raw pulses are significantly longer than the temporal window, the pulse width varies slowly when the window is slightly delayed forward or backward the peak.

In order to investigate the assumption of chirped pulses, optical fibre was used for compensation of the unfiltered output. As a result short pulses down to a picosecond and an RF peak increase by 10 dB could be measured with single mode (SM) fibre meaning that the raw pulses at the output of the laser were up-chirped. As shown in figure 12 the shortest pulse measured was obtained using 545 m of SM fibre (10.9 ps/nm). Assuming a sech^2 shape, the FWHM is ~975 fs after deconvolution and 1.06 ps .assuming Gaussian shape.

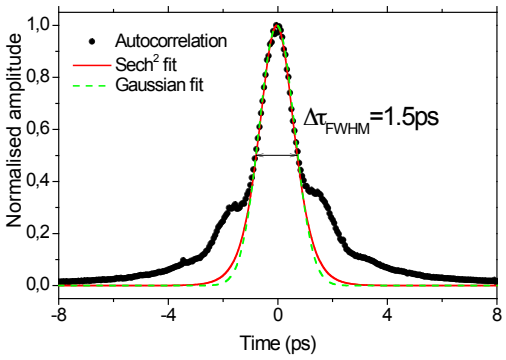

Figure 12: Autocorrelation trace (black dots) with sech^2 fit (red line) and Gaussian fit

τ_{FWHM}=1.5 ps; τ_{FWHM}/1.54=975 fs; $\tau_{FWHM}/\sqrt{2}$= 1.06ps

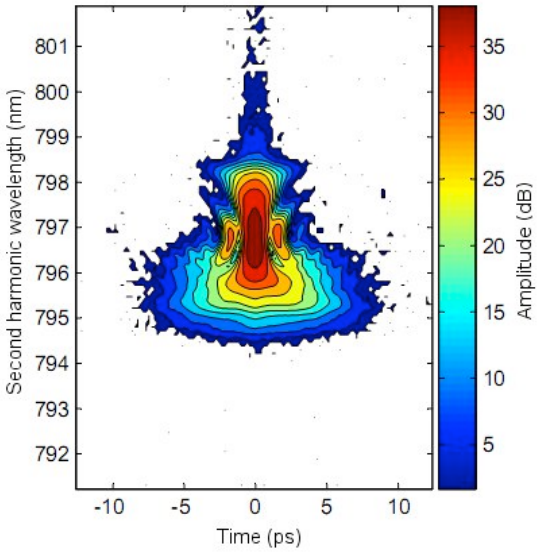

Figure 13: FROG trace

For both figures, the mode-locked laser output signal was sent through 545 m of SM fibre (250 mA in the gain section and SA 1.6 V reverse biased)

The transform limited pulse duration for the given spectral line width is 517 fs for the Gaussian shape. Since it is shorter than what was measured with nearly the optimum dispersion compensation it means that not all the lasing modes were locked into one regime of mode-locking which also fits well with the substructure seen in the optical spectrum. The spectral modulation but lack of temporal intensity modulation inside the laser means that the mode-locking mechanism cannot be described by the usual saturable absorber mode-locking but is rather akin to FM mode-locking through four-wave mixing [11, 12]. Therefore further investigation is needed so as to determine whether the analytical model could actually be applied for such cases, even though calculations are matching experimental observations. The autocorrelation trace in figure 12 exhibits a high pedestal confirming that the pulse is not transform limited. This pedestal seems to correspond to a pulse on the short wavelength side of the spectrum as seen on the frequency resolved optical gating (FROG) trace in figure 13.

Noise measurements were also carried out, the single sideband phase noise is -80 dBc/Hz at 100 kHz offset as seen on figure 14. This is about 20 dB lower than what was previously reported for single QW lasers [15]. The average jitter value is represented in figure 15 and is about 800 fs. This performance is mostly attributed to the low confinement factor induced by the use of QDH [7] and probably enhanced by the use of the double cap technique during the growth. Indeed as mentioned earlier the latter could allow the growth with fewer defects which are known to be a source of generation-recombination noise [26].

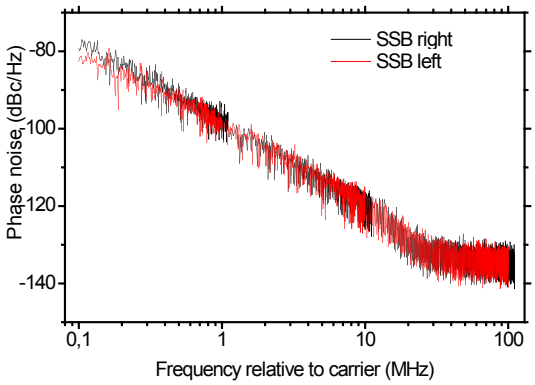

Figure 14: Single side band phase noise

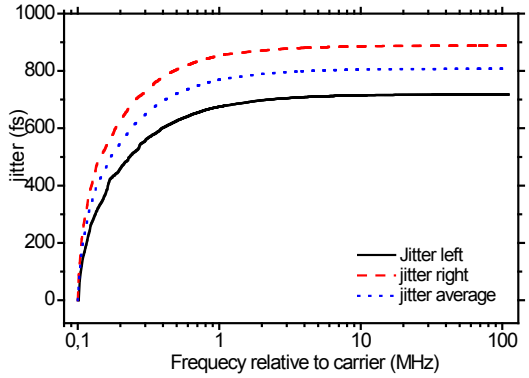

Figure 15: Jitter in left and right side of the carrier

4. CONCLUSION

Low noise and low threshold mode-locking operation has been demonstrated using a two-section InAs/InP QDH laser at 10.6 GHz. The interdependence of the device's geometry and the material parameters has been investigated with a theoretical model and found to be in agreement with measurements. Results show that the combination of a small absorbing section coupled to a high absorption coefficient can produce an efficient mode-locking. Experimental investigation showed that indeed short pulses could be obtained but the latter by using +10.9 ps/nm external dispersion compensation (about 545 m of SM fibre) meaning that the raw pulses are strongly up-chirped. Finally the single side band phase noise is about -80 dBc/Hz at 100 kHz offset and the average timing jitter is as low as 800 fs. This last point is particularly important for high precision digitization of very high frequency waveforms requiring sample clocks with extremely low timing jitter and low noise.

Acknowledgements

This work was supported by networks of Excellence ePIXnet and SANDIE and the Danish research council through the OPSCODER project.

We would like to thank Leif Oxenløwe and Michael Gallili for providing with equipments

REFERENCES

1. Van der Ziel, J. P., Tsang, W. T., Logan, R. A., Mikulyak, R. M., and Augustyniak, W. M. "Subpicosecond pulses from passively mode-locked GaAs buried optical guide semiconductor lasers," Applied Physics Letters 39, 7, (1981)
2. Silberberg, Y., Smith, P. W., Eilenberger, D. J., Miller, D. A. B., Gossard, A. C. and Wiegmann, W. "Passive mode-locking of a semiconductor diode-laser," Optics Express 9, 11, (1984)
3. Shimizu, T., Ogura, I., and Yokoyama, H., "860 GHz rate asymmetric colliding pulse modelocked diode lasers," Electronics Letters 33, 22, (1997)
4. Arakawa, Y., and Sakaki H., "Multidimensional quantum well laser and temperature dependence of its threshold current," Applied Physics Letters 40, 11, (1982)
5. Asada, M., Miyamoto, K., and Suematsu, Y., "Gain and the threshold of three-dimensional quantum-box lasers," IEEE Journal of Quantum Electronics. 22, 9, (1986)
6. Haus, H. A. "Modelocking of semiconductor laser diodes," Japanese Journal of Applied Physics 20, 1007, (1981)
7. Berg, T. W., and Mørk, J., "Quantum dot amplifiers with high output power and low noise," Applied Physics Letters 82, 18, (2003)
8. Huang, X., Stintz, A., Li, H., Lester L. F., Cheng, J., and Malloy, K. J. "Passive mode-locking in 1.3 μm two-section InAs quantum dot lasers," Applied Physics Letters 78, 19, (2001)

9. Thompson, M. G., Rae, A. R., Xia, M., Penty, R. V., and White, I. H. "InGaAs Quantum-Dot Mode-Locked Laser Diodes," IEEE Journal of Selected Topics in Quantum Electronics 15, 3, 661, (2009)
10. Novikov, I. I., Yu Gordeev, N., Maximov, M. V., Shernyakov, Y. M., Zhukov, A. E., Vasil'ev, A. P., Semenova, E. S., Ustinov, V. M., Ledentsov, N., N., Bimberg, D., Zakharov, N. D., and Werner, P., "Ultrahigh gain and non-radiative recombination channels in 1.5 μm range metamorphic InAs–InGaAs quantum dot lasers on GaAs substrates," Semiconductor Science and Technology 20, 33, (2005)
11. Merghem, K., Akrout, A., Martinez, A., Aubin, G., Ramdane, A., Lelarge, F., and Duan, G.-H., "Pulse generation at 346 GHz using a passively mode locked quantum-dash-based laser at 1.55 μm," Applied Physics Letters 94, 021107-1, (2009)
12. Lu, Z. G., Liu, J. R., Raymond, S., Poole, P. J., Barrios, P. J., and Poitras, D., "312-fs pulse generation from a passive C-band InAs/InP quantum dot mode-locked laser", Optics Express 16, 14, 10835, (2008)
13. Heck, M. J. R., Bente, E. A. J. M., Smalbrugge, B., Oei, Y-S., Smit, M. K., Anantathanasarn, S., and Nötzel, R., "Observation of Q-switching and mode-locking in two-section InAs/InP (100) quantum dot lasers around 1.55 μm," Optics Express 15, 25, 16292, (2007)
14. Heck, M. J. R., Renault, A., Bente, E. A. J. M., Oei, Y-S., Smit, M. K., Eikema, K. S. E., Ubachs, W., Anantathanasarn, S., and Nötzel, R., "Passively mode-locked 4.6 and 10.5 GHz quantum dot laser diodes around 1.55 μm with large operating regime", IEEE Journal of Selected Topics in Quantum Electronics 15, 3, 634, (2009)
15. Yvind, K., Larsson, D., Christiansen, L. J., Mørk, J., Hvam, J. M., and Hanberg, J. "High-performance 10GHz all-active monolithic modelocked semiconductor lasers", Electronics Letters. 40, 12, (2004)
16. Lin, C.-Y., Xin, Y.-C., Li, Y., Chiragh, F. L., and Lester, L. F., "Cavity design and characteristics of monolithic long- wavelength InAs/InP quantum dash passively mode-locked lasers," Optics Express 17, 22, (2009)
17. Paranthoen, C., Bertru, N., Dehaese, O., Le Corre, A., Loualiche, S., Lambert, B., and Patriarche, G., "Heigth dispersion control of InAs/InP quantum dots emitting at 1.55 μm," Applied Physics Letters 78, 12, 1751, (2001)
18. Hinooda, S., Fréchengues, S., Lambert, B., Loualiche, S., Paillard, M., Marie, X., and Amand, T., "Carrier dynamics of self-assembled InAs quantum dots on InP (311)B substrates," Applied Physics Letters 75, 22, 3530, (1999)
19. Miska, P., Even, J., Dehaese, O., and Marie, X., "Carrier relaxation dynamics in InAs/ InP quantum dots," Applied Physics Letters 92, 191103, (2008)
20. Homeyer, E., Piron, R., Grillot, F., Dehaese, O., Tavernier, K., Mace, E., Even, J., Lecorre, A., and Loualiche, S., "Demonstration of a Low Threshold Current in 1.54μm InAs/InP(311)B Quantum Dot Laser with Reduced Quantum Dot Stacks," Japanese Journal of Applied Physics, 46, 10A,6903, (2007)
21. Zhou, D., Piron, R., Dontabactouny, M., Dehaese, O., Grillot, F., Batte, T., Tavernier, K., Even, J., and Loualiche, S., "Low-threshold current density InAs quantum dash lasers on InP (100) grown by molecular beam epitaxy," Electronics Letters 45, 1, (2009)
22. Lau, K. Y., and Paslaski, J., "Condition for short pulse generation in ultrahigh frequency mode-locking of semiconductor-lasers" IEEE Photonics Technology Letters, vol. 3, 11, 974, 1991.
23. Palaski, J., and Lau, K. Y., "Parameter ranges for ultrahigh frequency mode-locking of semiconductor-lasers" Applied Physics Letters 59, 1, 7, (1991)
24. Xin, Y.-C., Li, Y., Martinez, A., Rotter, T. J., Su, H., Zhang, L., Gray, A. L., Luong, S., Sun, K. Zou, Z., Zilko, J., Varangis, P. M. and Lester, L. F. Optical gain and absorption of quantum dots measured using an alternative segmented contact method, Journal of Quantum Electronics 42, 7, 725, (2006)
25. Zhukov A. E., Kovsh, A. R., Ustinov, V. M., Egorov, A. Yu, Ledentsov, N. N., Tsatsul'nikov, A. F., Maximov, V. M., hernyakov, Yu M., Kopchatov, V. I., Lunev, A. V., Kop'ev, P. S., Bimberg D., and Alferov, Zh I., "Gain characteristics of quantum dot injection lasers" Semiconductor Science and Technology, vol. 14, 118, (1999)
26. Hu, G., Li, J., Shi, Y., and Shi, J., "The g-r noise in quantum well semiconductor lasers and its relation with device reliability," Optics and Laser Technology 39, 165, (2007)